Atmospheric Environment 63 (2012) 203–212

Contents lists available at SciVerse ScienceDirect

Atmospheric Environment

journal homepage: www.elsevier.com/locate/atmosenv

Formation of secondary organic carbon and long-range transport of carbonaceous aerosols at Mount Heng in South China

Shengzhen Zhou [a,b], Zhe Wang [a,b], Rui Gao [a], Likun Xue [a,b], Chao Yuan [a,b], Tao Wang [a,b,c,*], Xiaomei Gao [a], Xinfeng Wang [a,b], Wei Nie [a,b], Zheng Xu [a,b], Qingzhu Zhang [a], Wenxing Wang [a,c]

[a] Environment Research Institute, Shandong University, Ji'nan, Shandong 250100, PR China
[b] Department of Civil and Environmental Engineering, The Hong Kong Polytechnic University, Hong Kong, PR China
[c] Chinese Research Academy of Environmental Sciences, Beijing 100012, PR China

HIGHLIGHTS

- Characteristics of carbonaceous aerosols at Mount Heng in South China.
- SOC estimated from the EC-tracer method accounted for more than half of the total OC.
- In-cloud processing and acid-catalyzed reactions both contributed to SOA formation.
- Long-range transport of carbonaceous aerosol from PRD and eastern China was observed.
- Biomass burning emissions in Southeast Asia affected the air quality of South China.

ARTICLE INFO

Article history:
Received 28 May 2012
Received in revised form
10 September 2012
Accepted 12 September 2012

Keywords:
Carbonaceous aerosols
Secondary organic carbon (SOC)
Cloud processing
Acid-catalyzed reactions
Long-range transport

ABSTRACT

To understand the sources and formation processes of atmospheric carbonaceous aerosols in rural and mountainous areas of South China, an intensive measurement campaign was conducted at the summit of Mount Heng (27°18′N, 112°42′E, 1269 m asl) during the spring of 2009. The observed average concentrations of organic carbon (OC) and elemental carbon (EC) were 3.01 ± 2.2 and 0.54 ± 0.3 μg m^{-3}, respectively. The total carbonaceous aerosols (TCA) averagely contributed to 20.7% of $PM_{2.5}$. High OC/EC ratios (range: 1.6–10.4; average: 5.2 ± 1.8) were observed, suggesting the transport and secondary origins of the carbonaceous aerosols at Mount Heng. The amount of secondary organic carbon (SOC) was estimated using the EC-tracer method and accounted for 53.9% of the total OC on average. Good correlations were found between SOC and droplet-mode sulfate, and oxalate and droplet-mode sulfate, indicating the occurrence of in-cloud secondary organic aerosol (SOA) formation at Mount Heng. The concentrations of SOC and water soluble organic acids also displayed positive relationship with aerosol acidity, suggesting the enhancement of SOC formation by acid-catalyzed heterogeneous reactions. Backward trajectory analysis revealed that the observed aerosols at Mount Heng were predominantly associated with the air masses from the Pearl River Delta region (PRD) and Eastern China, which brought significant amounts of anthropogenic pollutants to the site. In addition, strong signals of biomass burning (elevated carbonaceous concentrations, OC/EC ratios and K^+ concentrations) were observed in air masses from Southeast Asia, demonstrating that the biomass burning emissions in Southeast Asia could reach the boundary layer of South China and affect the air quality there during the spring season.

1. Introduction

Atmospheric carbonaceous aerosols are major components of the fine particles in the troposphere, normally comprising 20–50% of the total fine aerosol mass, and up to 90% in tropical forested areas (Kanakidou et al., 2005). Carbonaceous aerosols have received increasing attention in recent years owing to their direct impacts on global radiation balance, climate change, public health and visibility reduction (Jacobson, 2001; Seinfeld and Pandis, 2006; Mauderly and Chow, 2008). Carbonaceous aerosols are operationally classified into three parts: organic carbon (OC), elemental carbon (EC), and carbonate carbon (CC). Compared to OC and EC, CC can normally be neglected due to its small mass contribution

* Corresponding author. Department of Civil and Environmental Engineering, The Hong Kong Polytechnic University, Hong Kong, PR China. Tel.: +852 2766 6059; fax: +852 2330 9071.
E-mail address: cetwang@polyu.edu.hk (T. Wang).

1352-2310/$ – see front matter © 2012 Elsevier Ltd. All rights reserved.
http://dx.doi.org/10.1016/j.atmosenv.2012.09.021

(Chow and Watson, 2002). EC (also termed BC) is formed as a byproduct of the incomplete combustion of fossil fuels and biomass, whereas OC can be either directly emitted from primary sources or formed through photochemical oxidation of volatile precursors (Seinfeld and Pandis, 2006).

Secondary organic aerosols (SOA) can account for 30–60% of the organic aerosols (OA) in urban air and more than 70% of the OA in rural air and the free troposphere (Volkamer et al., 2009). Recent studies have suggested that other SOA formation mechanisms, such as atmospheric aqueous-phase chemistry, are possibly important sources of SOA (Blando and Turpin, 2000; Yu et al., 2005). Some studies found that acid-catalyzed heterogeneous reactions on atmospheric aerosols can lead to significant increases in SOA mass in both the laboratory (Jang et al., 2002; Surratt et al., 2007) and in the field (Rengarajan et al., 2011). However, other studies found no apparent evidence for the enhancement of SOA in acidic aerosols (Peltier et al., 2007; Zhang et al., 2007). Heald et al. (2005) demonstrated a large gap between the measured and modeled organic aerosols and suggested that there are missing sources of SOA in the free troposphere. Due to this uncertainty in SOA formation, continuing field research on carbonaceous aerosols and SOA formation mechanisms under different atmospheric conditions is necessary.

Anthropogenic emissions of carbonaceous aerosols in Asia increased by 30% between 1980 and 2003 (Ohara et al., 2007). China, as one of the biggest contributors to Asian emissions, accounts for 49% and 62% of the total OC and EC emissions in this region (Zhang et al., 2009). Many studies on carbonaceous aerosols have been carried out in urban areas of developed regions in China (Yang et al., 2011). However, observations of carbonaceous aerosols in rural and mountain regions in China are still limited. Wang et al. (2011b) observed high concentrations of carbonaceous aerosols and predominant SOA formation at Mount Tai in the North China Plain, and Wang et al. (2011a) carried out observations at Mount Hua in North China. To our knowledge, observations and studies of carbonaceous aerosols in mountain areas in South China are still rare.

Mount Heng, a high altitude mountain (1269 m asl) located in the center of acid-rain affected South China (Fig. 1), is strongly influenced by the Asian Monsoon; the air masses that flow from the south and north alternate with each other frequently during the monsoon transition period in the spring season. The summit of Mount Heng could serve as a regionally representative site for studying the long range transport of aerosols and aerosol characteristics in an acidic atmosphere. Moreover, cloud and fog events often occur at the summit of Mount Heng, providing an opportunity for investigating SOA formation in clouds/fogs.

An extensive research project on aerosols, trace gases, cloud water and rain water was conducted at the summit of Mount Heng during the spring of 2009, as part of China's National Basic Research Project on acid rain. The ionic compositions of the aerosols are discussed in a separate paper (Gao et al., 2012). The present paper has three goals: (1) to study the concentrations and temporal variations of OC and EC in the $PM_{2.5}$ at Mount Heng; (2) to estimate secondary organic carbon (SOC) concentrations and to investigate possible heterogeneous SOA formation mechanisms; and (3) to examine the sources and transport patterns of the carbonaceous aerosols at Mount Heng.

2. Experiments

2.1. Site description and aerosol sampling

The field study was conducted at Mount Heng in Hunan province from March 15 to May 31, 2009. Mount Heng is a mountain range located in South China, about 1000 km and 600 km from Shanghai and Hong Kong, respectively (Fig. 1). The sampling site is situated at the Nanyue Mountain Weather Station at the summit of Mount Heng (27°18′N, 112°42′E, 1269 m asl). During the campaign, the daily average temperature varied from 2.2 to 20.8 °C, with monthly averages of 9.8, 12.2 and 16.3 °C in March, April and May, respectively. The daily average relative humidity (RH) varied from 47.5% to 100% in March, 52.1% to 100% in April, and 49.7% to 100% in

Fig. 1. Location of the Mount Heng site in South China.

May. More detailed information on the winds, precipitation and cloud events during this study can be found in Sun et al. (2010).

The $PM_{2.5}$ samples were collected by a four channels sampler (RAAS, Model: RAAS2.5-400, Thermo Anderson). Aerosols collected on 47-mm quartz microfiber filters (Pall corporation, USA; pre-fired at 600 °C for 6 h) in Channel 1 were used for the analysis of carbonaceous aerosols, and aerosols collected on Teflon-membrane filters (Pall corporation, USA) in Channel 2 were used for the determination of the mass concentrations, water-soluble inorganic ions and organic acid ions.

Normally the sampling period was 23.5 h, from 9:30 a.m. on one day to 9:00 a.m. the next day. Short-time samples were collected during dust storm episodes (6 h intervals) and daytime/nighttime samples (12 h intervals) were collected during May 1–21, 2009. After collection, the samples were stored in the refrigerator at −5 °C before being weighed and analyzed. In total, 95 valid samples with two sets of field blanks were obtained during the campaign. The filter samples were weighed using a Sartorius ME-5F balance (readability: 1 μg) before and after sampling at a constant temperature (20 ± 0.5 °C) and relative humidity (50% ± 2%) to determine their mass concentrations.

2.2. Analysis of carbonaceous species

A thermal–optical carbon aerosol analyzer (Sunset Laboratory) based on the thermal–optical transmittance (TOT) method (Birch and Cary, 1996) was used to determine the abundance of OC and EC with a modified NIOSH-5040 (National Institute of Occupational Safety and Health) protocol. The principles and the schematic of the instrument were depicted by Wang et al. (2011b). To ensure the accuracy of the OC and EC analysis, the analyzer was calibrated with a multipoint external standard calibration using the sucrose standard solution (slope: 1.03, $R^2 = 0.9998$) and CH_4 gas standard validations were performed periodically during the analysis. Oven cleaning procedures were implemented prior to analyzing the samples with the aim of checking the instrument blanks (Acceptance Criteria: Value ± 0.3 μg C). Two ambient blank filters were also analyzed for correcting the real ambient samples. The detection limit for OC and EC was 0.3 μg m^{-3} (Wang et al., 2011b), and the reproducibility was assessed by replicate analysis of samples, with uncertainty less than 5% for TC and 8% for OC and EC.

2.3. Analysis of aerosol acidity and relevant species

The aerosol acidity, $[H^+]_{air}$, was determined by two methods: measurement from water extracts of aerosol samples and calculated from thermodynamics model. Teflon-membrane filter samples were extracted ultrasonically in 20 ml deionized water (resistivity > 18.2 MΩ cm), and the pH value of the water extracts was determined using a pH meter (Shanghai Lei-Ci PHS-3C; Resolution: 0.01 pH). Then the $[H^+]_{air\text{-}extract}$ was calculated from the aqueous H^+ concentration in extraction and sampling air volume (Surratt et al., 2007).

The *in-situ* $[H^+]_{air}$ was calculated by Aerosol Inorganic Model (AIM-II) (Clegg et al., 1998). Inputs of the model included the concentrations of SO_4^{2-}, NO_3^- and NH_4^+ in $PM_{2.5}$, ambient temperature (T), relative humidity (RH) and calculated $[H]_{strong}$ ($[H]_{strong} = 2 \times [SO_4^{2-}] + [NO_3^-] - [NH_4^+]$) (Zhou et al., 2012).

Inorganic water-soluble ions (including F^-, Cl^-, NO_3^-, SO_4^{2-}, Na^+, NH_4^+, K^+, Ca^{2+} and Mg^{2+}) and water soluble organic acid anions (including lactate, acetate, formate, methane sulfonate and oxalate) were determined using Dionex IC 90 and Dionex IC 2500, respectively. More details of the measurement of ion species are described in Zhou et al. (2009). Relevant trace gases, such as SO_2, NO_y, O_3 and CO, were also measured simultaneously. The setup and description of these instruments were described in Wang et al. (2006).

3. Results and discussion

3.1. $PM_{2.5}$ carbonaceous aerosols at Mount Heng

The $PM_{2.5}$ mass concentration varied from 2.2 to 184.4 μg m^{-3}, with an average of 40.7 ± 30.9 μg m^{-3} during the campaign (Table 1). The average concentrations of OC and EC in the $PM_{2.5}$ were 3.01 and 0.54 μg m^{-3}, respectively. By using the nonurban OA/OC conversion ratio of 2.1 (Turpin and Lim, 2001), the average concentration of OA in the $PM_{2.5}$ was calculated to be 6.32 μg m^{-3} at Mount Heng. The contributions of different components in the $PM_{2.5}$ during the dust storm and non-dust storm periods are depicted in Fig. 2. As shown, SO_4^{2-}, NO_3^- and NH_4^+ ions were the dominant constituents of the water soluble ions. OA constituted 8.3% and 18.8% of the $PM_{2.5}$ during dust storm and non-dust periods, respectively. The reduced contributions of soluble ions and carbonaceous species during the dust storms were due to the unidentified insoluble crust materials shown as "others" (71.9%) in the Fig. 2. Table 2 compares the carbonaceous aerosol concentrations at the Mount Heng site with other high-altitude and rural background sites. Although the sizes of the particulate matter in those studies are different, the comparisons are logical as OC and EC mainly exist in fine particles (Offenberg and Baker, 2000). The observed concentrations of OC and EC in $PM_{2.5}$ at Mount Heng were higher than the concentrations at remote sites in China, such as Zhuzhang in southwest China and Muztagh Ata in northwest China, but were lower than those in the Daihai site and the Mount Tai site in North China. The carbonaceous concentrations at Mount Heng are apparently higher than those at mountain sites in Europe and America, but lower than those at Manora Peak (India) and Kathmandu valley (Nepal) in South Asia during the spring season.

Temporal variations of OC, EC, $PM_{2.5}$, trace gases and meteorological parameters during the campaign are depicted in Fig. 3. As shown, OC and EC exhibited similar temporal variations, suggesting they had common sources and underwent similar atmospheric processes for most of the observation period. Diurnal differences in OC and EC concentrations were also observed during May 1–21, 2009, with much higher concentrations in the daytime (4.61 and 0.79 μg m^{-3}) than in the nighttime (2.21 and 0.43 μg m^{-3}, respectively). As can be seen from Fig. 3, massive dust storms were observed on March 22 and on April 25–26 at Mount Heng, with the highest 1-h PM_{10} and $PM_{2.5}$ concentrations of 524.3 μg m^{-3}, 200.5 μg m^{-3} and 911.2 μg m^{-3}, 289.2 μg m^{-3} during the two

Table 1
Statistics of the abundances of EC, OC, TCA and $PM_{2.5}$ at Mount Heng in the spring of 2009.

	EC (μg m^{-3})	OC (μg m^{-3})	OC/EC ratio	TCA (μg m^{-3})	$PM_{2.5}$ (μg m^{-3})	OC/$PM_{2.5}$ (%)	EC/$PM_{2.5}$ (%)	TCA/$PM_{2.5}$ (%)
Ave	0.54	3.01	5.2	6.9	40.7	9.4	1.9	20.7
Max	1.4	11.5	10.4	25.6	184.4	33.3	7.2	47.6
Min	BDL[a]	BDL	1.6	BDL	2.2	BDL	BDL	BDL
SD	0.3	2.2	1.8	4.8	30.9	5.5	1.3	8.9

[a] BDL: below detection limit.

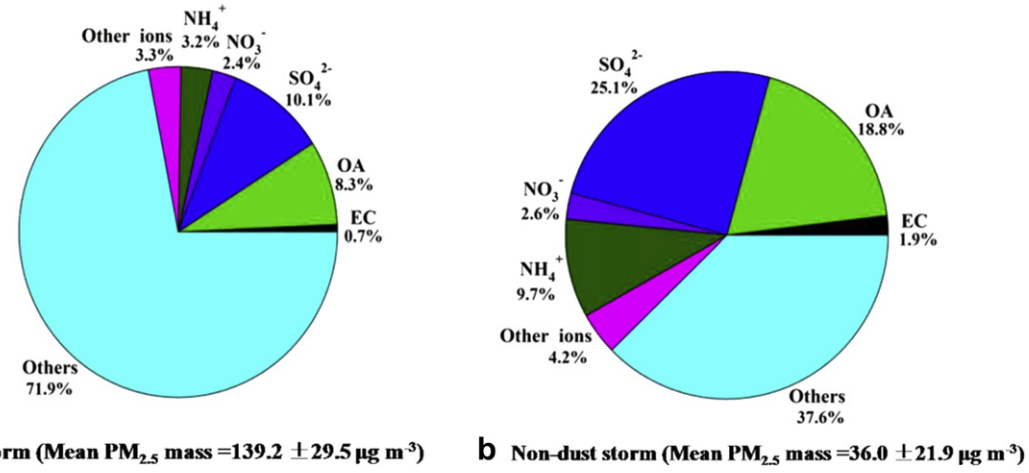

Fig. 2. The chemical compositions of $PM_{2.5}$ during (a) dust storm periods (March 22 and April 25–26) and (b) non-dust storm periods in the spring of 2009. Other ions include F^-, Cl^-, Na^+, K^+, Ca^{2+} and Mg^{2+}; OA = 2.1 × OC.

periods, respectively. OC and EC concentrations also increased during the dust storms, indicating that the dust plumes had mixed with anthropogenic pollution during transport. It is worth noting that much higher OC and EC concentrations were observed during March 18–21, 2009, as well as high K^+ concentrations, suggesting the presence of emissions from biomass burning (further discussed in Section 3.3). During May 7–9, OC concentrations and OC/EC ratio (8.3) were also high, consistent with the high O_3 concentrations (the highest 1-h O_3 concentration of 114.6 ppb), indicating the photochemical production of SOA.

The relationship between OC and EC can provide useful insights into the origin of carbonaceous aerosols (Turpin and Huntzicker, 1995). A good correlation ($R = 0.87$, $p < 0.0001$) was observed between OC and EC in the $PM_{2.5}$ at Mount Heng (Fig. 4), suggesting common emission sources for OC and EC. The OC/EC ratios at Mount Heng varied from 1.6 to 10.4, with an average of 5.2 in this campaign (Table 1). This is comparable to the OC/EC ratio of 5.0 at Mount Tai in the spring of 2007 in North China (Wang et al., 2011b) and those of the other rural and mountain sites listed in Table 2, indicating the presence of aged aerosols from long-range transport. OC/EC ratios exceeding 2 (Chow et al., 1996) or 2.2 (Turpin and Huntzicker, 1995) have been used to identify the presence of secondary organic aerosol. The average OC/EC ratio (5.2) at Mount Heng was much higher than 2.2 and the urban ratios observed in China (e.g., 2.9 in Beijing, 2.5 in Shanghai, and 2.4 in PRD (Cao et al., 2003; Yang et al., 2005)), suggesting that SOA may make a large contribution to the organic aerosols at Mount Heng.

3.2. Secondary organic aerosol (SOA) formation

3.2.1. Estimation of secondary organic carbon (SOC) concentration

The EC-tracer method was used to estimate the SOC concentration at Mount Heng. Based on the approach proposed by Turpin and Huntzicker (1995), SOC can be obtained by:

$$OC_{sec} = OC_{tot} - OC_{pri} \quad (1)$$

and

$$OC_{pri} = EC \times (OC/EC)_{pri} \quad (2)$$

where OC_{sec} is the secondary OC, OC_{tot} is the total OC, OC_{pri} denotes the primary OC, and $(OC/EC)_{pri}$ is the primary OC/EC ratio.

The crucial step in this method is the selection of the primary OC/EC ratio, as it can vary between sources and is influenced by the meteorology, diurnal and seasonal fluctuations in emissions, etc. Data with OC/EC ratio below the threshold of 2.9 or in the lowest 5–10% have been used to determine the primary OC/EC ratio from least-square regression (Strader et al., 1999; Lim and Turpin, 2002). In this study, we selected data with OC/EC ratio in the lowest 10% and without significant influence from rain and cloud. The regression of the selected data suggested a primary OC/EC ratio of 2.2, which was comparable with 2.19 at Mount Tai in North China (Wang et al., 2011c). Analyses of trace gas and other aerosol data at Mount Heng indeed indicate reduced photochemical activities in

Table 2
Comparisons of EC and OC concentrations, and OC/EC ratios among various high-altitude and rural background sites around the world.

Location	Size	asl (m)	Time period	EC (μg m^{-3})	OC (μg m^{-3})	OC/EC	Analysis method	Reference
Mount Heng, China (27.3°N, 112.7°E)	$PM_{2.5}$	1269	Ma–May 2009	0.54	3.01	5.2	TOT[a]	This study
Mount Tai, China (36.3°N, 117.1°E)	$PM_{2.5}$	1533	Mar–Apr 2007	1.77	6.07	5.0	TOT	(Wang et al., 2011b)
Daihai, China (40.6°N, 112.6°E)	TSP	1221	Apr–May 2007	1.81	8.1	5	TOR[b]	(Han et al., 2007)
Zhuzhang, China (28.0°N, 99.7°E)	PM_{10}	3580	Jul 2004–Mar 2005	0.34	3.13	11.9	TOR	(Qu et al., 2009)
Muztagh Ata, China (38.3°N, 75.0°E)	TSP	4500	Mar–May 2004 and Mar–May 2005	0.038	0.36	12.0	TOR	(Cao et al., 2009)
Kathmandu, Nepal (27.7°N, 85.5°E)	PM_{10}	2150	Feb–May 2000	1.5	14.37		TOT	(Carrico et al., 2003)
Manora Peak, India (29.4°N, 79.5°E)	TSP	1950	Feb–Mar 2005	1.8	11.6	6.6	TOT	(Ram et al., 2008)
Mount Zirkel, USA (40.8°N, 106.7°E)	$PM_{2.5}$	3224	Dec 1994–Nov 1995	0.27	1.05		TOR	(Watson et al., 2001)
Puy de Dome, France (45.8°N, 2.95°E)	PM_{10}	1450	Apr–Sep 2004	0.26	2.4	10.6	TOT	(Pio et al., 2007)
Sonnblick, Austria (47.0°N, 13.0°E)	$PM_{2.5}$	3106	May–Jun 2003	0.23	1.38	7.9	TOT	(Pio et al., 2007)
Jungfraujoch, Switzerland (46.6°N, 8.0°E)	$PM_{2.5}$	3580	Jul–Aug 1998	0.29	1.05	3.57	A&C[c]	(Krivacsy et al., 2001)

[a] TOT: thermal–optical transmittance.
[b] TOR: thermal–optical reflectance.
[c] A&C: Aethalometer (BC) and combustion methods (TOC); Therefore, OC = combustion (TOC) − Aethalometer (BC).

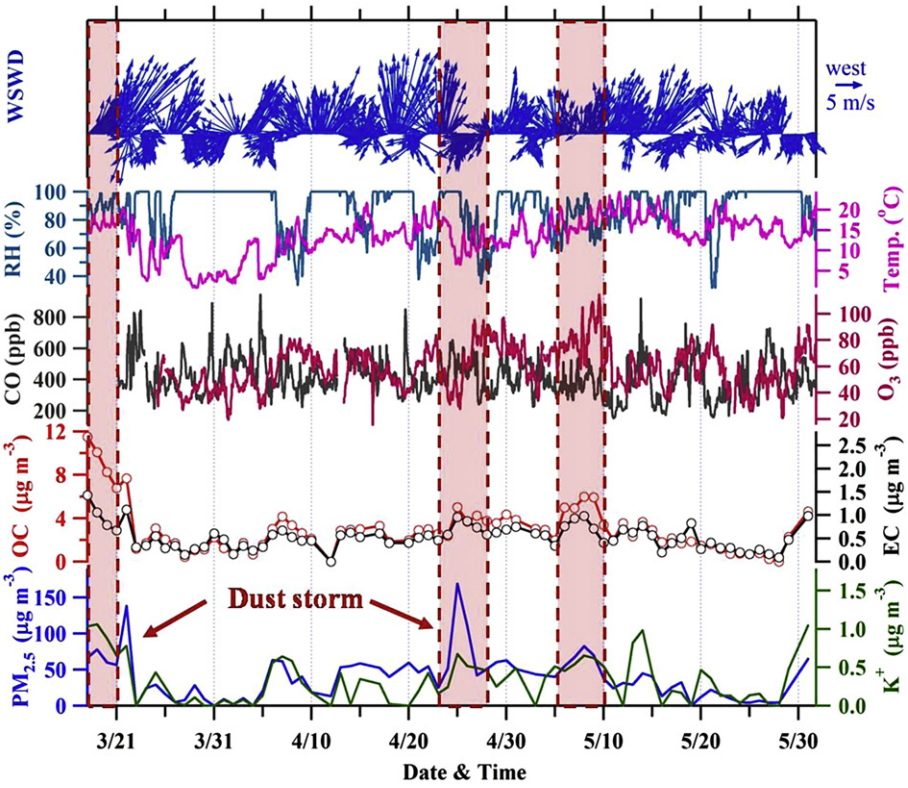

Fig. 3. Temporal variations of OC, EC, K^+ and $PM_{2.5}$ concentrations, trace gases and meteorological parameters from March 18 to May 31, 2009 at Mount Heng.

the periods of the lowest OC/EC ratios. For example, the average mixing ratio of ozone was 45.2 (±7.1) ppb for the lowest 10% OC/EC data, compared to 60.9 (±13.9) ppb for the whole period; CO, a trace gas from primary emissions, was 505 (±91) ppb, compared to 401 (±84) ppb. In addition, the sum of the five organic acid anions (including lactate, acetate, formate, methane sulfonate and oxalate), which are mostly formed through secondary process and considered as a proxy for the SOA (e.g., Rengarajan et al., 2011), also showed much lower mean concentration for the period of lowest 10% OC/EC ratios (0.08 μg m^{-3} versus 0.42 μg m^{-3}). Despite the apparent reduced photochemistry in the periods of lowest 10% OC/EC ratios, some chemical transformation may still occur in these air masses when pollutants at surface were transported to the mountain-top site, thus the estimated primary OC/EC ratio of 2.2 is likely to be an upper limit of the 'average' ratio of primary emissions in the region. As a result, the calculated SOC using this method may represent a lower bound of the abundance of the SOC. Additional uncertainty may arise from our use of the same primary OC/EC emission ratio for air masses transported from different regions.

The calculated SOC concentrations varied from 0 to 8.36 μg m^{-3}, with an average of 1.85 μg m^{-3}. The contribution of SOC to the total OC ranged from 0 to 78.9% with an average of 53.9%. Daytime and nighttime SOC concentrations in May 2009 were 2.9 ± 1.5 and 1.3 ± 1.0 μg m^{-3} respectively, accounting for 60.1% and 49.9% of the total OC, indicating that more SOA were formed from photochemical production during the daytime. Moreover, a much higher SOC concentration was observed during the photochemical pollution episode on May 9 (Fig. 3), during which the SOC accounted for as much as 73.5% of the total OC. Biomass burning emissions have a much higher primary OC/EC ratio than other sources, which can cause the overestimation of SOC. Considering the possible impact of biomass burning, we excluded the data collected between March 18–21 from our determination of the SOC concentration. The derived SOC concentration, without the biomass burning influence, was 1.52 μg m^{-3}, accounting for 52.4% of the total OC.

3.2.2. SOA formation in cloud/fog processing

Though clouds and fogs may scavenge aerosols and result in a decrease in aerosol concentration, it has been suggested by previous laboratory and field studies that aqueous-phase reactions

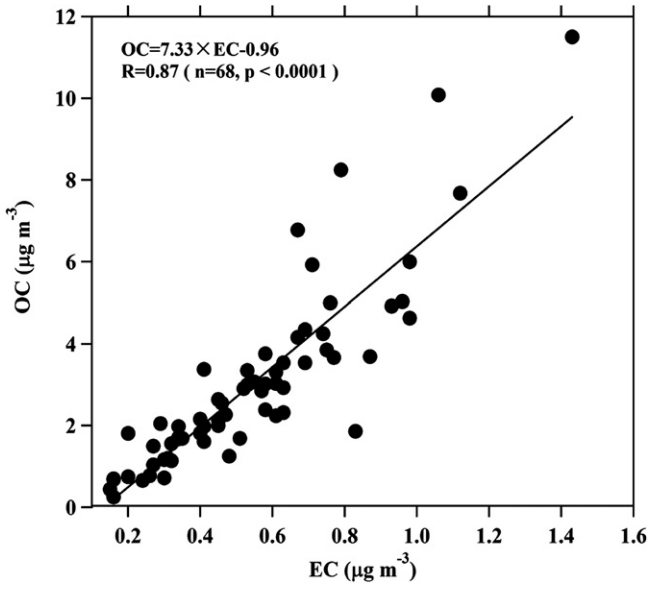

Fig. 4. Scatter plot of OC and EC concentrations in $PM_{2.5}$ at Mount Heng.

in cloud/fog processing could be an important pathway for SOA formation (De Haan et al., 2011; Wang et al., 2011c). Taking advantage of the frequent cloud/fog events during the campaign in Mount Heng, we selected daily samples of cloud/fog events (without rain) lasting over 6 h to investigate the relationship between cloud/fog and carbonaceous aerosols. It is well known that the droplet mode (aerodynamic diameter around 0.5–1 μm) of SO_4^{2-} is formed through the aqueous oxidation of SO_2 in clouds (Meng and Seinfeld, 1994; Seinfeld and Pandis, 2006). During our field study at Mount Heng, sulfate showed a single peak in the size bin of 0.56–1.0 μm, indicating the important role of aqueous-phase oxidation of SO_2 gas to aerosol SO_4^{2-} (Gao et al., 2012). The relationship between SO_4^{2-} and SOC in aerosol during the cloudy/foggy days at Mount Heng is depicted in Fig. 5. As shown, sulfate and SOC correlated well ($R = 0.87$, $p < 0.001$) when the regression equation of $SOC = 0.18 \times [SO_4^{2-}] - 0.22$ was applied. This result suggests that the sulfate and SOC may have gone through similar cloud/fog processing.

Particulate OC is a mixture of hundreds of individual constituents with a wide range of chemical and thermodynamic properties. Oxalic acid is typically the most abundant dicarboxylic acid in organic aerosols, and chamber experiments have shown that oxalic acid could also be formed in cloud/fog processing (Carlton et al., 2007). Five carboxylic acid anions were measured during the campaign at Mount Heng, and Fig. 6 shows the correlation between sulfate and oxalate in the aerosols ($R = 0.83$, $p < 0.001$). This correlation indicates a common in-cloud source for these two chemically distinct species. Similar close tracking of these two species was also observed in several urban and coastal sites in China (Yao et al., 2002; Yu et al., 2005), suggesting the potential importance of in-cloud processing on oxalate formation. Considering the frequent clouds at the summit and favorable sampling conditions, the positive correlation between oxalate and sulfate at Mount Heng provides more direct evidence for the in-cloud formation pathway of oxalate and SOA.

Fig. 7 shows the temporal variation of SOC concentrations with related species during a cloud/fog event observed on April 29–30. A heavy cloud/fog started in the morning of April 29 and lasted until the afternoon of April 30. It can be seen in the Fig. 7 that the

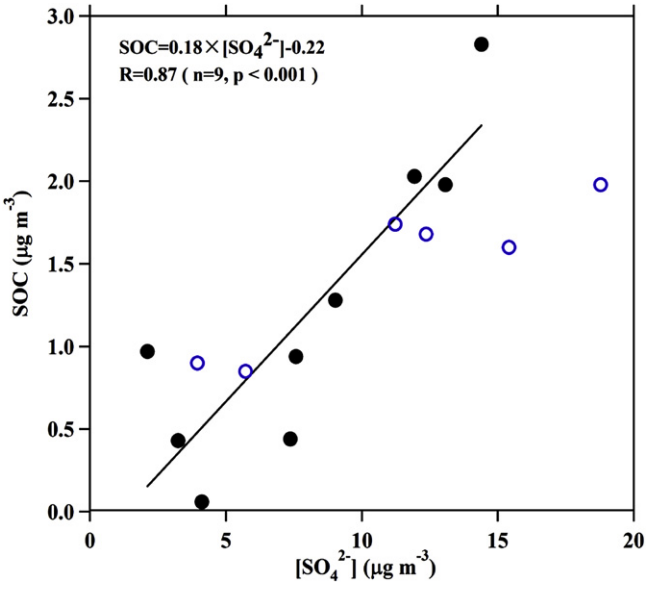

Fig. 5. Scatter plot of SOC and sulfate concentrations in $PM_{2.5}$ during cloud/fog events in the spring of 2009. The solid circles denote the samples with cloud/fog processing over 6 h ($n = 9$); the open circles denote the samples with cloud/fog processing less than 6 h ($n = 6$).

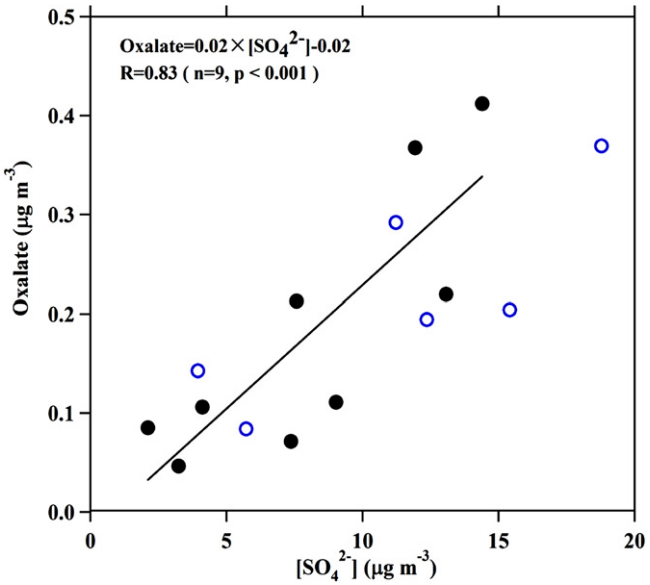

Fig. 6. Scatter plot of oxalate and sulfate concentrations in $PM_{2.5}$ during cloud/fog events in the spring of 2009. The solid circles denote the samples with cloud/fog processing over 6 h ($n = 9$); the open circles denote the samples with cloud/fog processing less than 6 h ($n = 6$). The regression slop is calculated for samples with cloud/fog processing over 6 h.

concentrations of SOC, sulfate, and oxalate all increased after the cloud/fog processing. Acetate, which was reported to be one of the intermediates of in-cloud isoprene chemistry for the formation of hygroscopic oxalic acids (Lim et al., 2005), was also enhanced, demonstrating the substantial SOA formation through cloud processing at Mount Heng.

3.2.3. Aerosol acidity and SOA

The measured pH values of the aerosol water extracts ranged from 4.3 to 5.9 (with an average of 4.9), and corresponding hydrogen ion concentration $[H^+]_{air\text{-}extract}$ varied from 0 to 56.8 nmol m^{-3} with an average of 18.7 nmol m^{-3}, demonstrating the overall acidic character of the fine particles at Mount Heng. The modeled *in-situ* $[H^+]_{air}$ from AIM-II model ranged from 0.5 to 7.2 nmol m^{-3}, and was lower than but well correlated with the measured $[H^+]_{air\text{-}extract}$. This is consistent with the results of Rengarajan et al. (2011), who reported lower modeled $[H^+]_{air}$ by about 2 orders of magnitude than the measured data and similarity in their variability. The modeled $[H^+]_{air}$ derived from the thermodynamic gas–aerosol equilibrium system based on measured ionic compositions was considered as a more accurate indicator of aerosol acidity.

The relationship between aerosol acidity ($[H^+]_{air}$) and SOA formation was investigated at Mount Heng. In order to avoid the influences of other atmospheric processes, such as cloud/fog processing, photochemical reaction, dust storms and biomass burning, filter samples collected on days with O_3 mixing ratios of less than 80 ppb and without clouds, dust storm or biomass burning were selected. As can be seen in Fig. 8a, the higher SOC concentrations are associated with increased *in-situ* $[H]_{air}$ concentrations, and liner regression analysis suggests a good correlation ($R = 0.70$, $p < 0.01$) with the linear relation of $SOC = 0.32 \times [H^+]_{air} + 0.75$. Water soluble organic carbon (WSOC), which is represented by the sum of the five organic acid anions, also showed a positive correlation with aerosol acidity ($R = 0.85$, $p < 0.01$), with the linear relation of $WSOC = 0.067 \times [H^+]_{air} + 0.13$ (Fig. 8b). These results indicate that heterogeneous acid-catalyzed reactions may have contributed to SOA formation during our observation period.

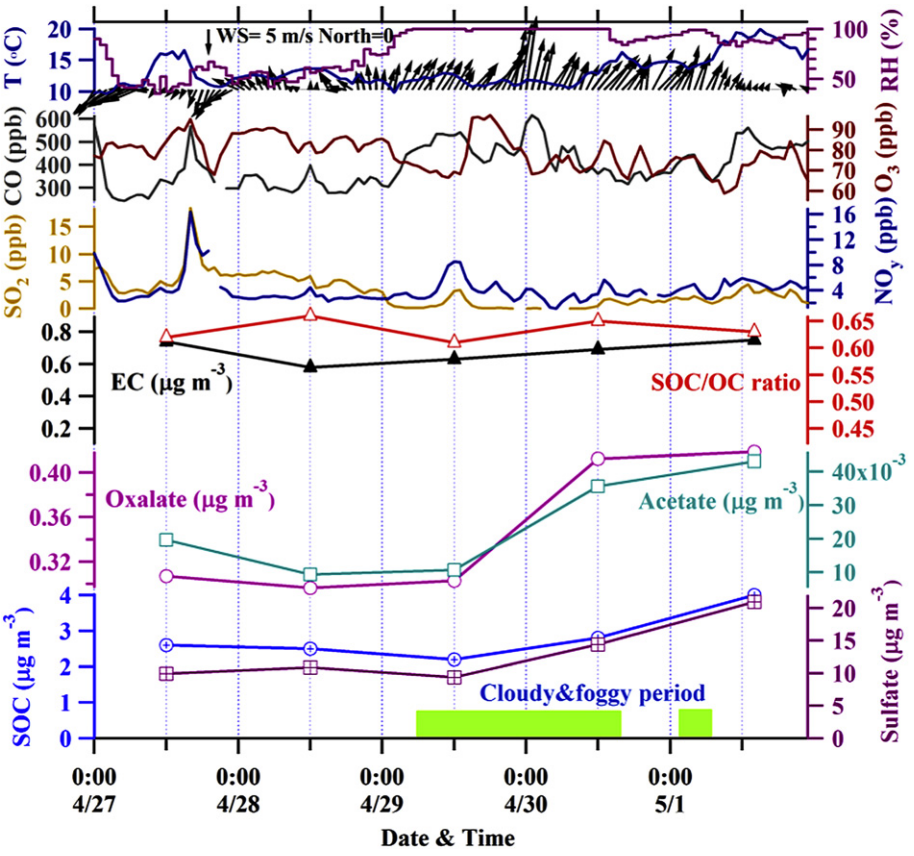

Fig. 7. Time series of the concentrations of SOC, sulfate, oxalate, acetate, trace gases (O_3, SO_2, NO_y and CO), and meteorological parameters during a typical cloud/fog event observed from April 28 to May 1, 2009 at Mount Heng.

The SOC–$[H^+]_{air}$ slope (0.32) at Mount Heng is higher than that (0.15) observed in an urban environment in western India by Rengarajan et al. (2011), and also higher than the observed increment of SOC (0.0389 μg per nmol m^{-3} $[H^+]$) produced from isoprene in a laboratory chamber study (Surratt et al., 2007) and the results from α-pinene and β-caryophyllene (0.0035–0.022 μg SOC per nmol m^{-3} $[H^+]$) (Offenberg et al., 2009).

3.3. Transport pattern and sources of carbonaceous aerosols

To better understand the origins and the transport patterns of the sampled air masses, five-day back trajectories at the altitude of 1300 m asl were calculated using the Hybrid Single Particle Lagrangian Integrated Trajectory (HYSPLIT Model, version 4.9) (Draxler and Rolph, 2003). Due to the scavenging and formation processes that occurred in cloud/fog conditions, the samples collected during cloud/fog periods were excluded from the trajectory analysis. A cluster analysis was performed to segregate the data set of the calculated trajectories into distinct groups as described by Xue et al. (2011). Fig. 9 shows the derived five trajectory clusters together with an occurrence percentage for each trajectory cluster. The five clusters were classified according to directions as North China Gobi (NG), Northwest China (NWC), Southeast Asia (SEA), Pearl River Delta (PRD), and North and Eastern China (NEC). Among the five identified trajectory clusters, NEC and PRD were the most frequent, and each accounted for 28%

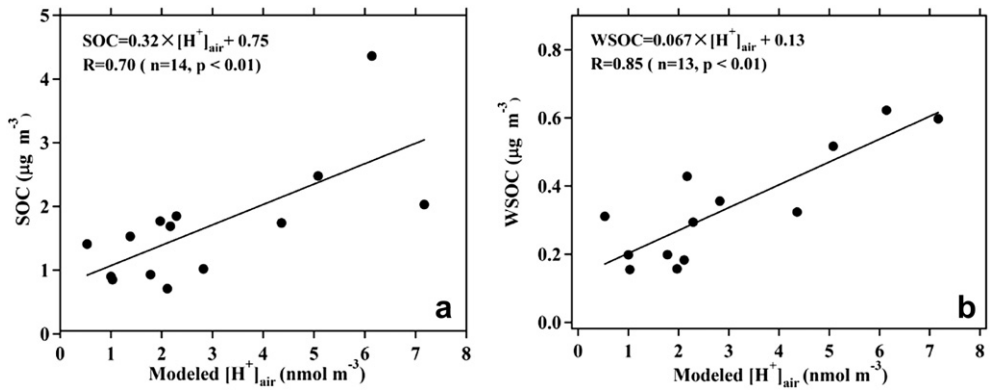

Fig. 8. Scatter plot of (a) SOC and modeled $[H^+]_{air}$ concentration and (b) WSOC and modeled $[H^+]_{air}$ concentration during the spring of 2009 at Mount Heng.

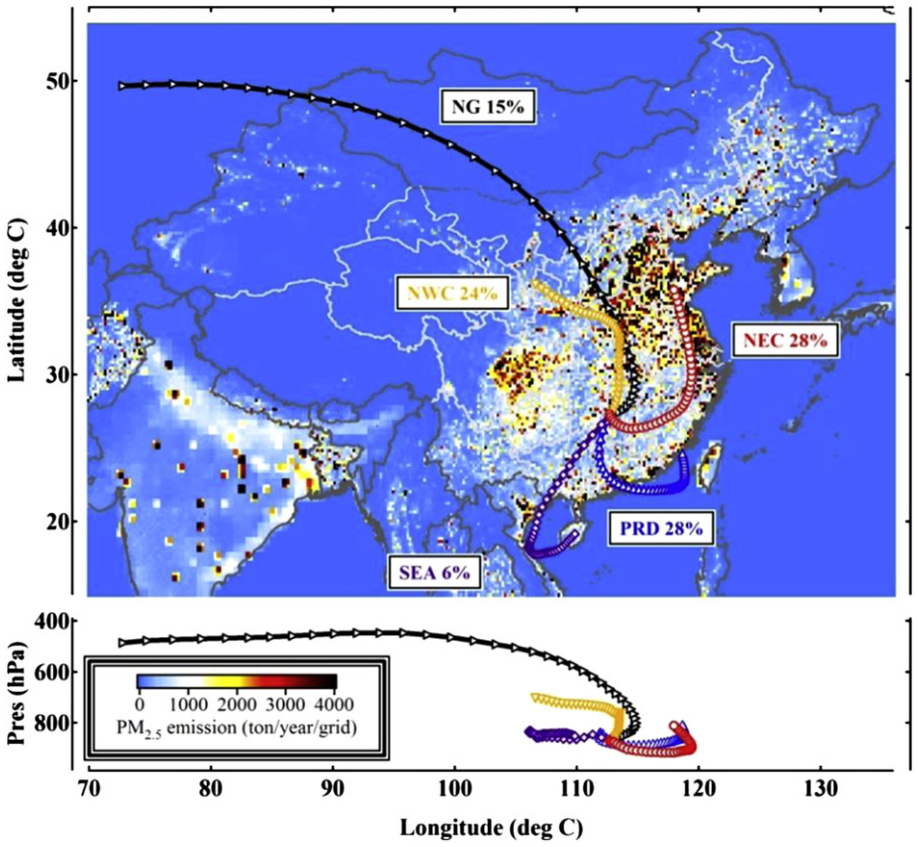

Fig. 9. Five-day air mass trajectory clusters at Mount Heng during the campaign. Also shown is the girded $PM_{2.5}$ emission in 2006 from Zhang et al. (2009).

of the total air masses, followed by NWC (24%), NG (15%) and SEA (6%). The statistical summary of carbonaceous concentrations for each transport cluster is listed in Table 3.

The $PM_{2.5}$ mass concentration showed the highest values in the NG cluster trajectories due to the frequent dust storm events during the spring season in North China. The order of carbonaceous concentrations among the clusters was SEA > NG > NEC > PRD > NWC, and the sequence of OC/EC ratios is SEA > PRD > NEC > NWC > NG (Table 3). Unexpectedly, the highest OC and EC concentration (9.16 and 0.99 μg m^{-3}, respectively) were associated with the air mass from the SEA cluster. The highest OC/EC ratio was also observed in this group, with an average of 9.5. Cachier et al. (1989) found an OC/EC ratio of 9.0 in biomass burning in a tropical area. The high OC/EC ratio recorded in this study may suggest that the air masses from the SEA cluster were impacted by biomass burning.

The SEA trajectories originated from Southeast Asia (see in Fig. 9), and they mainly occurred in March 18–21. It is known that extensive biomass burning occurs in Southeast Asia each year from January to May, peaking in March (Duncan et al., 2003). Fig. 10 shows back trajectories and fire spots (obtained from http://firefly.geog.umd.edu/firemap/) during March 15–21, demonstrating that the air masses that arrived at Mount Heng had passed over the areas of Southeast Asia with intensive fire spots. The trajectory result is further supported by the high concentration of the biomass burning tracer K^+ collected during this period (Fig. 3). These results indicate that the byproducts of biomass burning in Southeast Asia in the spring can be transported to the boundary layer of South China, resulting in a sharp rise of aerosol concentrations and bad air quality.

The majority of the air masses observed during the study were from the PRD and NEC regions, which accounts for 56% of the total air mass. They had passed over the highly polluted regions of China (i.e., PRD and Eastern China). The average concentrations of OC and EC for air masses from PRD and NEC were 3.56, 0.53 μg m^{-3} and 3.72, 0.59 μg m^{-3}, respectively, with high SOC contributions to the OC. The frequent occurrence of these air masses and the relatively high concentrations of carbonaceous aerosols indicate the important impact that pollution sources in PRD and Eastern China have on carbonaceous material (and other aerosol components) via

Table 3
Percentage of occurrence of trajectory, mean concentrations of OC, EC, SOC and $PM_{2.5}$, and OC/EC ratios for each trajectory cluster at Mount Heng during the spring of 2009.

Air mass	% of total (%)	Mean concentration, μg m^{-3}				OC/EC ratio	$OC/PM_{2.5}$ (%)	$EC/PM_{2.5}$ (%)	SOC	SOC/OC (%)
		EC	OC	TCA	$PM_{2.5}$					
NEC	28%	0.59	3.72	8.39	52.24	6.2	6.9%	1.1%	2.42	64.4%
PRD	28%	0.53	3.56	8.01	43.12	6.6	8.2%	1.3%	2.38	63.8%
NWC	24%	0.54	2.98	6.78	51.51	5.3	6.9%	1.3%	1.79	57.6%
NG	15%	0.72	3.69	8.48	68.40	5.2	6.8%	1.3%	2.10	57.0%
SEA	6%	0.99	9.16	20.21	65.19	9.5	14.0%	1.5%	6.98	76.7%

NEC: North and Eastern China; PRD: Pearl River Delta region; NWC: Northwest China; NG: North China Gobi; SEA: Southeast Asia.

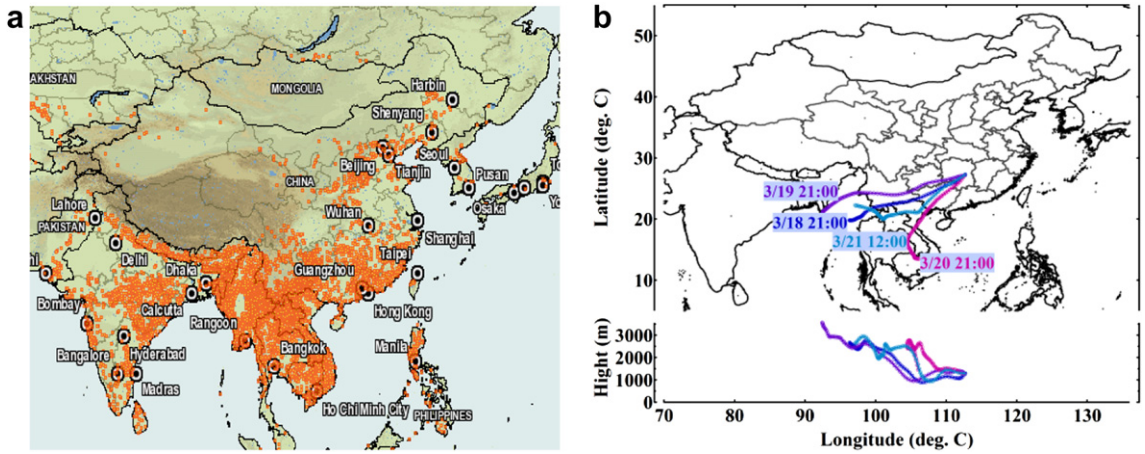

Fig. 10. (a) Geographical distribution of fires from March 15–21, 2009 (http://firefly.geog.umd.edu/firemap/) and (b) 3-day backward trajectories started at local time 21:00 March 18, 21:00 March 19, 21:00 March 20 and 12:00 March 21 at the altitude of 1300 m.

long-range transport. In comparison, the NWC air masses, which came from relatively clean northwest regions and originated in the free troposphere, had the lowest carbonaceous aerosol concentration (6.78 μg m^{-3}).

4. Summary and conclusions

$PM_{2.5}$ carbonaceous aerosols were investigated at Mount Heng in the spring of 2009. The mean concentrations of OC, EC and $PM_{2.5}$ were 3.01, 0.54, 40.7 μg m^{-3}, respectively. TCA accounted for 9.0% and 20.7% of the $PM_{2.5}$ in dust storm and non-dust storm periods, respectively. The estimated average SOC concentration was 1.85 μg m^{-3} (1.52 μg m^{-3} for non-biomass burning period), accounting for more than half of the OC mass at Mount Heng. Increased concentrations of sulfate, water soluble organic acids and SOC were observed during cloud/fog events with a good correlation between droplet-mode sulfate and SOC, indicating the occurrence of in-cloud SOA formation at Mount Heng. The positive relationship between aerosol acidity and SOC suggests the enhancement of SOC by acid-catalyzed heterogeneous reactions. During the study period, the majority of air masses arriving at Mount Heng had passed over the highly polluted coastal regions of China (the PRD and the eastern coast), demonstrating the impact of the long-range transport of pollutants from these developed regions on the rural areas of southern China. Strong signals of biomass burning in SE Asia were observed in air masses originating from that region in the early stage of the study, with the highest average organic carbon. More studies are warranted on the extent of the impact of the biomass burning on regional air quality and on the chemistry and radiation budget of the atmosphere in southern China.

Acknowledgments

The authors would like to thank Qiang Ma, Yangchun Yu, Sun Minghu and Linlin Wang for their help in sample collection, Yan Wang, Aijun Ding and Shaojia Fan for their help in the field study, and Weijun Li for his useful comments. The authors thank the Mount Heng Meteorological Observatory for their support during the field study and NOAA Air Resources Laboratory (ARL) for making available the HYSPLIT trajectory model. The authors are also grateful to the two anonymous reviewers for their helpful comments and suggestions on the manuscript. This work is supported by the National Basic Research Project of China (973 Project No. 2005CB422203) and the Niche Area Development Program of the Hong Kong Polytechnic University (1-BB94).

References

Birch, M., Cary, R., 1996. Elemental carbon-based method for monitoring occupational exposures to particulate diesel exhaust. Aerosol Science and Technology 25 (3), 221–241.
Blando, J.D., Turpin, B.J., 2000. Secondary organic aerosol formation in cloud and fog droplets: a literature evaluation of plausibility. Atmospheric Environment 34 (10), 1623–1632.
Cachier, H., Brémond, M.P., Buat-Ménard, P., 1989. Carbonaceous aerosols from different tropical biomass burning sources. Nature 340, 371–373.
Cao, J., Lee, S., Ho, K., Zhang, X., Zou, S., Fung, K., Chow, J., Watson, J., 2003. Characteristics of carbonaceous aerosol in Pearl River Delta Region, China during 2001 winter period. Atmospheric Environment 37 (11), 1451–1460.
Cao, J., Xu, B., He, J., Liu, X., Han, Y., Wang, G., Zhu, C., 2009. Concentrations, seasonal variations, and transport of carbonaceous aerosols at a remote mountainous region in western China. Atmospheric Environment 43 (29), 4444–4452.
Carlton, A.G., Turpin, B.J., Altieri, K.E., Seitzinger, S., Reff, A., Lim, H.J., Ervens, B., 2007. Atmospheric oxalic acid and SOA production from glyoxal: results of aqueous photooxidation experiments. Atmospheric Environment 41 (35), 7588–7602.
Carrico, C., Bergin, M., Shrestha, A., Dibb, J., Gomes, L., Harris, J., 2003. The importance of carbon and mineral dust to seasonal aerosol properties in the Nepal Himalaya. Atmospheric Environment 37 (20), 2811–2824.
Chow, J., Watson, J., Lu, Z., Lowenthal, D., Frazier, C., Solomon, P., Thuillier, R., Magliano, K., 1996. Descriptive analysis of $PM_{2.5}$ and PM_{10} at regionally representative locations during SJVAQS/AUSPEX. Atmospheric Environment 30 (12), 2079–2112.
Chow, J., Watson, J., 2002. $PM_{2.5}$ carbonate concentrations at regionally representative interagency monitoring of protected visual environment sites. Journal of Geophysical Research-Atmospheres 107 (D21), 8344 . http://dx.doi.org/10.1029/2001JD000574.
Clegg, S.L., Brimblecombe, P., Wexler, A.S., 1998. Thermodynamic model of the system H^+–NH_4^+–SO_4^{2-}–NO_3–H_2O at tropospheric temperatures. The Journal of Physical Chemistry A 102 (12), 2137–2154.
De Haan, D.O., Hawkins, L.N., Kononenko, J.A., Turley, J.J., Corrigan, A.L., Tolbert, M.A., Jimenez, J.L., 2011. Formation of nitrogen-containing oligomers by methylglyoxal and amines in simulated evaporating cloud droplets. Environmental Science & Technology 45 (3), 984–991.
Draxler, R., Rolph, G., 2003. HYSPLIT (HYbrid Single-particle Lagrangian Integrated Trajectory) Model, NOAA Air Resources Laboratory. Silver Spring, MD. Access via NOAA ARL READY Website. http://www.arl.noaa.gov/ready/hysplit4.html.
Duncan, B., Martin, R., Staudt, A., Yevich, R., Logan, J., 2003. Interannual and seasonal variability of biomass burning emissions constrained by satellite observations. Journal of Geophysical Research-Atmospheres 108 (D2), 4100. http://dx.doi.org/10.1029/2002JD002378.
Gao, X., Xue, L., Wang, X., Wang, T., Yuan, C., Gao, R., Zhou, Y., Nie, W., Zhang, Q., Wang, W., 2012. Aerosol ionic components at Mt. Heng in central southern China: abundances, size distribution, and impacts of long-range transport. Science of the Total Environment 433, 498–506.
Han, Y., Han, Z., Cao, J., Chow, J., Watson, J., An, Z., Liu, S., Zhang, R., 2007. Distribution and origin of carbonaceous aerosol over a rural high-mountain lake area, Northern China and its transport significance. Atmospheric Environment 42, 2405–2414.

Heald, C.L., Jacob, D.J., Park, R.J., Russell, L.M., Huebert, B.J., Seinfeld, J.H., Liao, H., Weber, R.J., 2005. A large organic aerosol source in the free troposphere missing from current models. Geophysical Research Letters 32 (18), L18809. http://dx.doi.org/10.1029/2005GL023831.

Jacobson, M., 2001. Strong radiative heating due to the mixing state of black carbon in atmospheric aerosols. Nature 409 (6821), 695–697.

Jang, M., Czoschke, N.M., Lee, S., Kamens, R.M., 2002. Heterogeneous atmospheric aerosol production by acid-catalyzed particle-phase reactions. Science 298 (5594), 814–817.

Kanakidou, M., Seinfeld, J., Pandis, S., Barnes, I., Dentener, F., Facchini, M., Van Dingenen, R., Ervens, B., Nenes, A., Nielsen, C., 2005. Organic aerosol and global climate modelling: a review. Atmospheric Chemistry and Physics 5 (4), 1053–1123.

Krivacsy, Z., Hoffer, A., Sarvari, Z., Temesi, D., Baltensperger, U., Nyeki, S., Weingartner, E., Kleefeld, S., Jennings, S., 2001. Role of organic and black carbon in the chemical composition of atmospheric aerosol at European background sites. Atmospheric Environment 35 (36), 6231–6244.

Lim, H., Turpin, B., 2002. Origins of primary and secondary organic aerosol in Atlanta: results of time-resolved measurements during the Atlanta supersite experiment. Environmental Science & Technology 36 (21), 4489–4496.

Lim, H.J., Carlton, A.G., Turpin, B.J., 2005. Isoprene forms secondary organic aerosol through cloud processing: model simulations. Environmental Science & Technology 39 (12), 4441–4446.

Mauderly, J.L., Chow, J.C., 2008. Health effects of organic aerosols. Inhalation Toxicology 20 (3), 257–288.

Meng, Z., Seinfeld, J.H., 1994. On the source of the submicrometer droplet mode of urban and regional aerosols. Aerosol Science and Technology 20 (3), 253–265.

Offenberg, J., Baker, J., 2000. Aerosol size distributions of elemental and organic carbon in urban and over-water atmospheres. Atmospheric Environment 34 (10), 1509–1517.

Offenberg, J.H., Lewandowski, M., Edney, E.O., Kleindienst, T.E., Jaoui, M., 2009. Influence of aerosol acidity on the formation of secondary organic aerosol from biogenic precursor hydrocarbons. Environmental Science & Technology 43 (20), 7742–7747.

Ohara, T., Akimoto, H., Kurokawa, J., Horii, N., Yamaji, K., Yan, X., Hayasaka, T., 2007. An Asian emission inventory of anthropogenic emission sources for the period 1980–2020. Atmospheric Chemistry and Physics 7 (3), 4419–4444.

Peltier, R., Sullivan, A., Weber, R., Wollny, A., Holloway, J., Brock, C., de Gouw, J., Atlas, E., 2007. No evidence for acid-catalyzed secondary organic aerosol formation in power plant plumes over metropolitan Atlanta, Georgia. Geophysical Research Letters 34 (6), L06801. http://dx.doi.org/10.1029/2006GL028780.

Pio, C., Legrand, M., Oliveira, T., Afonso, J., Santos, C., Caseiro, A., Fialho, P., Barata, F., Puxbaum, H., Sanchez-Ochoa, A., 2007. Climatology of aerosol composition (organic versus inorganic) at nonurban sites on a west–east transect across Europe. Journal of Geophysical Research-Atmospheres 112, D23S02. http://dx.doi.org/10.1029/2006JD008038.

Qu, W., Zhang, X., Arimoto, R., Wang, Y., Wang, D., Sheng, L., Fu, G., 2009. Aerosol background at two remote CAWNET sites in western China. Science of the Total Environment 407 (11), 3518–3529.

Ram, K., Sarin, M., Hegde, P., 2008. Atmospheric abundances of primary and secondary carbonaceous species at two high-altitude sites in India: sources and temporal variability. Atmospheric Environment 42 (28), 6785–6796.

Rengarajan, R., Sudheer, A., Sarin, M., 2011. Aerosol acidity and secondary organic aerosol formation during wintertime over urban environment in western India. Atmospheric Environment 45 (11), 1940–1945.

Seinfeld, J., Pandis, S., 2006. Atmospheric Chemistry and Physics: From Air Pollution to Climate Change. John Wiley & Sons, New York.

Strader, R., Lurmann, F., Pandis, S., 1999. Evaluation of secondary organic aerosol formation in winter. Atmospheric Environment 33 (29), 4849–4863.

Sun, M., Wang, Y., Wang, T., Fan, S., Wang, W., Li, P., Guo, J., Li, Y., 2010. Cloud and the corresponding precipitation chemistry in South China: water-soluble components and pollution transport. Journal of Geophysical Research-Atmospheres 115 (D22), D22303. http://dx.doi.org/10.1029/2010JD014315.

Surratt, J.D., Lewandowski, M., Offenberg, J.H., Jaoui, M., Kleindienst, T.E., Edney, E.O., Seinfeld, J.H., 2007. Effect of acidity on secondary organic aerosol formation from isoprene. Environmental Science & Technology 41 (15), 5363–5369.

Turpin, B., Huntzicker, J., 1995. Identification of secondary organic aerosol episodes and quantitation of primary and secondary organic aerosol concentrations during SCAQS. Atmospheric Environment 29 (23), 3527–3544.

Turpin, B., Lim, H., 2001. Species contributions to $PM_{2.5}$ mass concentrations: revisiting common assumptions for estimating organic mass. Aerosol Science and Technology 35 (1), 602–610.

Volkamer, R., Ziemann, P., Molina, M., 2009. Secondary Organic Aerosol Formation from Acetylene (C_2H_2): seed effect on SOA yields due to organic photochemistry in the aerosol aqueous phase. Atmospheric Chemistry and Physics 9 (6), 1907–1928.

Wang, G., Li, J., Cheng, C., Hu, S., Xie, M., Gao, S., Zhou, B., Dai, W., Cao, J., An, Z., 2011a. Observation of atmospheric aerosols at Mt. Hua and Mt. Tai in central and east China during spring 2009 – part 1: EC, OC and inorganic ions. Atmospheric Chemistry and Physics. 11 (9), 4221–4235.

Wang, T., Wong, H., Tang, J., Ding, A., Wu, W., Zhang, X., 2006. On the origin of surface ozone and reactive nitrogen observed at a remote mountain site in the northeastern Qinghai-Tibetan Plateau, western China. Journal of Geophysical Research-Atmospheres 111 (D8), D08303. http://dx.doi.org/10.1029/2005JD006527.

Wang, Z., Wang, T., Gao, R., Xue, L., Guo, J., Zhou, Y., Nie, W., Wang, X., Xu, P., Gao, J., 2011b. Source and variation of carbonaceous aerosols at Mount Tai, North China: results from a semi-continuous instrument. Atmospheric Environment 45 (9), 1655–1667.

Wang, Z., Wang, T., Guo, J., Gao, R., Xue, L., Zhang, J., Zhou, Y., Zhou, X., Zhang, Q., Wang, W., 2011c. Formation of secondary organic carbon and cloud impact on carbonaceous aerosols at Mount Tai, North China. Atmospheric Environment 46, 516–527.

Watson, J., Chow, J., Lowenthal, D., Cahill, C., Blumenthal, D., Richards, L., Jorge, H., 2001. Aerosol chemical and optical properties during the Mt. Zirkel visibility study. Journal of Environmental Quality 30 (4), 1118–1125.

Xue, L., Wang, T., Zhang, J., Zhang, X., 2011. Source of surface ozone and reactive nitrogen speciation at Mount Waliguan in western China: new insights from the 2006 summer study. Journal of Geophysical Research-Atmospheres 116 (D7), D07306. http://dx.doi.org/10.1029/2010JD014735.

Yang, F., He, K., Ye, B., Chen, X., Cha, L., Cadle, S., Chan, T., Mulawa, P., 2005. One-year record of organic and elemental carbon in fine particles in downtown Beijing and Shanghai. Atmospheric Chemistry and Physics 5, 1449–1457.

Yang, F., Tan, J., Zhao, Q., Du, Z., He, K., Ma, Y., Duan, F., Chen, G., 2011. Characteristics of $PM_{2.5}$ speciation in representative megacities and across China. Atmospheric Chemistry and Physics 11, 5207–5219.

Yao, X., Fang, M., Chan, C.K., 2002. Size distributions and formation of dicarboxylic acids in atmospheric particles. Atmospheric Environment 36 (13), 2099–2107.

Yu, J., Huang, X., Xu, J., Hu, M., 2005. When aerosol sulfate goes up, so does oxalate: implication for the formation mechanisms of oxalate. Environmental Science & Technology 39 (1), 128–133.

Zhang, Q., Jimenez, J.L., Worsnop, D.R., Canagaratna, M., 2007. A case study of urban particle acidity and its influence on secondary organic aerosol. Environmental Science & Technology 41 (9), 3213–3219.

Zhang, Q., Streets, D.G., Carmichael, G.R., He, K., Huo, H., Kannari, A., Klimont, Z., Park, I., Reddy, S., Fu, J., 2009. Asian emissions in 2006 for the NASA INTEX-B mission. Atmospheric Chemistry and Physics 9 (14), 5131–5153.

Zhou, Y., Wang, T., Gao, X., Xue, L., Wang, X., Wang, Z., Gao, J., Zhang, Q., Wang, W., 2009. Continuous observations of water-soluble ions in $PM_{2.5}$ at Mount Tai (1534 m asl) in central-eastern China. Journal of Atmospheric Chemistry 64, 107–127.

Zhou, Y., Xue, L., Wang, T., Gao, X., Wang, Z., Wang, X., Zhang, J., Zhang, Q., Wang, W., 2012. Characterization of aerosol acidity at a high mountain site in central eastern China. Atmospheric Environment 51, 11–20.